Non-Markovianity of an atom in a semi-infinite rectangular waveguide

Jing Zeng(曾静)[1], Yaju Song(宋亚菊)[2], Jing Lu(卢竞)[1], and Lan Zhou(周兰)[1,†]

[1] *Key Laboratory of Low-Dimensional Quantum Structures and and Quantum Control of the Ministry of Education, Department of Physics and Synergetic Innovation Center of Quantum Effects and Applications, Key Laboratory for Matter Microstructure and Function of Hunan Province, Hunan Normal University, Changsha* 410081, *China*

[2] *College of Physics and Electronic Engineering, Hengyang Normal University, Hengyang* 421002, *China*

(Received 1 November 2022; revised manuscript received 11 December 2022; accepted manuscript online 16 December 2022)

We investigate the non-Markovianity (NM) of a waveguide QED with a two-level atom as the system and a semi-infinite rectangular waveguide as the environment, where the transverse magnetic (TM_{mn}) modes define the quantum channels of guided photons. The perfect mirror imposed by the finite end exerts a retarded feedback mechanism to allow for information backflow, which leads to NM dynamics. For the energy separation of the atom far away from the cutoff frequencies of transverse modes, the delay differential equations are obtained with single-excitation initial in the atom. Our attention is focused on the effects of multiple quantum channels involved in guiding photons on the degree of non-Markovian behavior. An asymptotic value of the non-Markovianity $\mathcal{N}_1$ can be found as the atom–mirror distance is large enough, however, the asymptotic value of $\mathcal{N}_2$ of the atom interacting with the effective double-modes is lower than that of the atom interacting with the effective single-mode. We also show that $\mathcal{N}_1$ is a constant, and the analytical expression for $\mathcal{N}_2$ is related to the parameters associated with the modes, which is related to the interference of the two modes.

Keywords: open system, non-Markovianity, waveguide QED, quantum information

PACS: 03.65.Yz, 32.80.Qk, 42.50.–p, 03.67.–a **DOI:** 10.1088/1674-1056/acac18

1. Introduction

In the last decade, experimental progress opens up a new area for the study of the interaction between (natural or artificial) atoms and a continuum of propagating photonic modes, called waveguide quantum electromagnetic dynamics (QED).[1–6] Compared with cavity QED, waveguides offer an easier way for information transport due to the nonlocality of electromagnetic field. By virtue of its advantage in extensibility and integrability, waveguide QED becomes a promising candidate for quantum network,[3] quantum communication,[7–10] and quantum simulation.[11] Until now, a great many experimental implementations of one-dimensional (1D) waveguide QED have been developed, including those systems based on optical fibers,[12,13] photonic crystals,[14–17] plasmons,[18–20] and superconductors.[7,21–28]

The atomic spontaneous emission (SE)[29] is a key research topic in waveguide QED. The SE can be manipulated through environment engineering.[30–32] In free space, the atomic excited-state population decays irreversibly, and the probability of the emitted photon being reabsorbed is negligible. But in a structured environment, the modified electromagnetic field modes lead to the reversible decay process of atomic excited-state population. Moreover, the memory effects in structured environments can be quantified by non-Markovianity. Based on the divisibility of the dynamical map describing the time evolution of open system, the irreversible decay in spontaneous emission corresponds to Markovian dynamics, while the quantum revival corresponds to non-Markovian dynamics.[33–35] Recently, many different kinds of non-Markovianity measure have been proposed.[36–38] Here we adopt the definition based on the amount of information exchange between the open system and its environment.[39–42] Furthermore, recent research has extended to more complex non-Markovian systems, such as driven system,[43] spin chains,[44] and two excitation subspaces.[45]

In this paper we study a two-level atom interacting with the field modes of a semi-infinite rectangular waveguide, where the finite end is assumed to be a perfect mirror. The photon emitted by the atom undergoes back-reflection by the mirror,[46–49] which makes a flow of information back to the two-level atom. A waveguide with a cross section has multiple transverse modes with different cut-off frequencies,[50,51] *e.g.*, transverse-magnetic (TM) modes or transverse-electric (TE) ones. The larger cross-section area, the more transverse modes involved in the atomic interaction. However, most work only consider atoms interacting with one guiding mode of the waveguide. The SE of an atom and the entanglement of two atoms in a waveguide with cross section have been studied in Refs. [52–54]. Here we investigate the influence of the atom–mirror distance on the non-Markovianity of the atom with the single excitation initially. When the energy separation of the atom is far away from the cutoff frequencies of the transverse modes, the delay differential equations are obtained for the

†Corresponding author. E-mail: zhoulan@hunnu.edu.cn

© 2023 Chinese Physical Society and IOP Publishing Ltd

atomic amplitude. Although the SE is dependent on the delay times and phases which are induced by the atom–mirror distance, the environmental memory time is characterized by the delay times. The non-Markovianity (NM) is analyzed based on the information backflow when the atom interacts with either single transverse mode or double transverse modes of the waveguide.

This paper is organized as follows. In Section 2, we introduce the system we consider, and derive the delay differential equation describing the atomic SE in single excitation space under the premise of linearized dispersion relation. In Section 3, we first briefly introduce the measure of non-Markovianity, and the influence of the atom–mirror distance on the non-Markovianity and their regulation mechanism in both single-transverse mode and multi-transverse modes cases are studied. Finally, a summary is given in Section 4.

2. Physical model and dynamical evolution

As shown in Fig. 1, the setup under consideration is a waveguide-QED system consisting of a two-level atom and a semi-infinite rectangular waveguide with cross sectional area $A = ab$. The waveguide is formed by perfect mirrors at $x = 0, a$, $y = 0, b$, and $z = 0$, which support photons to travel in two types of propagation modes: transverse electric (TE) modes and transverse magnetic (TM) modes.[50,51,53] The wave vector $\boldsymbol{k}$ can be characterized by $(m\pi/a, n\pi/b, k)$ with integers m and n. The wave number k along the z direction is a continuous variable. Therefore, the waveguide allows a continuous range of frequencies described by the dispersion relation $\omega_{mnk} = \sqrt{\Omega_{mn}^2 + c^2k^2}$, where c is the light speed in vacuum, $\Omega_{mn} = \pi c\sqrt{m^2/a^2 + n^2/b^2}$ is the cutoff frequency. Notice that m and n cannot both be zero, otherwise, the atom will decouple to the field. If $a < b$ ($2a = b$), TE_{01} is the lowest propagation mode for the waveguide to interact with atoms, and the corresponding lowest TM mode occurs for $m = 1$, $n = 1$. Obviously, each propagation mode provides a quantum channel for photons to travel.

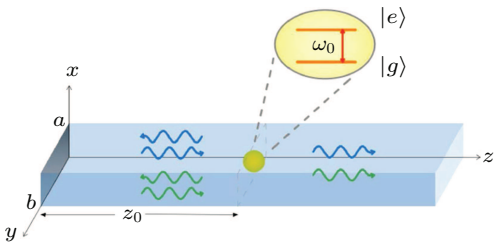


Fig. 1. Schematic diagram for a semi-infinite rectangular waveguide coupled to a two-level atom with transition frequency ω_0 at $\boldsymbol{r} = (a/2, b/2, z_0)$. The cross-section area of the waveguide is $A = ab$ ($2a = b$) parallel to the x–y plane.

A two-level atom with the transition frequency ω_0 is placed at $\boldsymbol{r} = (x_0, y_0, z_0)$ in the waveguide. z_0 is the distance between the atom and the termination at $z = 0$. Denoting the two internal states of this atom as the excited state $|e\rangle$ and the ground state $|g\rangle$, we can define the atomic rising (lowering) operator $\hat{\sigma}_+ \equiv |e\rangle\langle g|$ ($\hat{\sigma}_- \equiv |g\rangle\langle e|$). For simplification, we consider the atomic electric dipole is oriented along the z direction, which means that the atom only couple to the TM electric field via the dipole interaction. Since the number (m,n,k) specifies the mode function of this waveguide, we label the annihilation (creation) operator for each TM mode by $a_{mnk}^{(\dagger)}$. The total Hamiltonian (with $\hbar = 1$) $H = H_0 + H_\mathrm{I}$ of the hybrid system is given by the free Hamiltonian

$$H_0 = \omega_0 |e\rangle\langle e| + \sum_{mn}\int_{-\infty}^{\infty} \mathrm{d}k\,\omega_{mnk} a_{mnk}^\dagger a_{mnk}, \tag{1}$$

and the interaction Hamiltonian between the atom and field in the electric-dipole and rotating-wave approximation,

$$H_\mathrm{I} = \sum_{mn}\int_{-\infty}^{\infty} \mathrm{d}k\, g_{mnk}(\sigma_- a_{mnk}^\dagger - \sigma_+ a_{mnk}), \tag{2}$$

where mode-dependent coupling strength

$$g_{mnk} = \mathrm{i}\frac{g_0}{\sqrt{\omega_{mnk}}}\Omega_{mn}\sin\frac{m\pi}{2}\sin\frac{n\pi}{2}\cos(kz_0) \tag{3}$$

with $g_0 \equiv 2d\sqrt{\pi A\varepsilon_0}$. Here, the parameter ε_0 is the vacuum permittivity, and the matrix element d of the atomic dipole transition is set to be real. Obviously, the atom located at $x_0 = a/2$ and $y_0 = b/2$ decouples to the TM_{mn} mode with even integer m or n. In order to remove the high frequency oscillation of the system wavefunction, we express the total Hamiltonian in the interaction picture with respect to the free Hamiltonian H_0 as

$$H' = \sum_{mn}\int_{-\infty}^{\infty} \mathrm{d}k\, g_{mnk}\sigma_- a_{mnk}^\dagger\, \mathrm{e}^{-\mathrm{i}(\omega_0-\omega_{mnk})t} + \mathrm{H.c.} \tag{4}$$

The excitation number is conserved in this waveguide-QED system, *i.e.*, $[H,N] = 0$ with $N \equiv |e\rangle\langle e| + \sum_{mn}\int \mathrm{d}k\, a_{mnk}^\dagger a_{mnk}$, then the wavefunction of the total system in single-excitation subspace reads

$$|\psi(t)\rangle = e(t)|e0\rangle + \sum_{mn}\int_{-\infty}^{\infty} \mathrm{d}k\,\varphi_{mn}(k,t)\, a_{mnk}^\dagger |g0\rangle. \tag{5}$$

where $e(t)$ is the amplitude for the atom in the excited state with no photons in the field, and $\varphi_{mn}(k,t)$ is the amplitude for the atom in the ground state accompanied by an emitted photon with frequency ω_{mnk}. The initial state is denoted by the amplitudes $e(0) = 1$ and $\varphi_{mn}(k,0) = 0$. With the use of Schrödinger equation $\mathrm{i}\frac{\mathrm{d}}{\mathrm{d}t}|\psi(t)\rangle = H'|\psi(t)\rangle$, we obtain a set of coupled differential equations for the amplitudes

$$\begin{aligned} \dot{e}(t) &= \mathrm{i}\sum_{mn}\int \mathrm{d}k\, g_{mnk}\varphi_{mn}(k,t)\,\mathrm{e}^{\mathrm{i}(\omega_0-\omega_{mnk})t}, \\ \dot{\varphi}_{mn} &= -\mathrm{i}g_{mnk}e(t)\,\mathrm{e}^{-\mathrm{i}(\omega_0-\omega_{mnk})t}. \end{aligned} \tag{6}$$

The evolution of atomic excitation population is usually analyzed by tracing out the field modes. Then, we formally integrate the equation of $\dot{\varphi}_{mn}(k,t)$, which is later inserted into

the equation of $\dot{e}(t)$. The probability amplitude for the excited atomic state is determined by the following integro-differential equation

$$\dot{e}(t) = -\sum_{mn}\int \mathrm{d}k \int_0^t \mathrm{d}\tau e(\tau)\left|g_{mnk}\right|^2 \mathrm{e}^{\mathrm{i}\Delta_{mnk}(\tau-t)}, \tag{7}$$

where $\Delta_{mnk} = \omega_{mnk} - \omega_0$ is the detuning of ω_0 and ω_{mnk}. The above equation shows that the value of $\dot{e}(t)$ depends on the values of $e(t)$ at all earlier time. By assuming that the transition frequency ω_0 is far away from the cut-off frequencies Ω_{mn}, the photon frequency ω_{mnk} can be expanded around the ω_0 up to the linear term

$$\omega_{mnk} \approx \omega_0 + \upsilon_{mn}(k - k_{mn0}), \tag{8}$$

where $k_{mn0} = \sqrt{\omega_0^2 - \Omega_{mn}^2}/c$ is determined by $\omega_{mnk_0} = \omega_0$, and the photon group velocity in TM_{mn} mode is

$$\upsilon_{mn} \equiv \left.\frac{\partial \omega_{mnk}}{\partial k}\right|_{k=k_{mn0}}.$$

We further assume that the spectral density of the field around the atomic resonance is flat, that is, $g_0/\sqrt{\omega_{mnk}} \approx g_0/\sqrt{\omega_0}$. Substituting Eq. (8) into the integro-differential equation (7), integrating over k gives rise to a linear combination of $\delta(t \pm \tau_{mn} - \tau)$ and $\delta(t-\tau)$, where $\tau_{mn} = 2z_0/\upsilon_{mn}$ is the time delay taking by an emitted photon traveling back from the mirror in the given TM_{mn} mode. We obtain a delay-differential equation

$$\dot{e}(t) = -\sum_{mn}\left[\frac{\gamma_{mn}}{2}e(t) + \frac{\gamma_{mn}}{2}\mathrm{e}^{\mathrm{i}\phi_{mn}}e(t-\tau_{mn})\,\theta(t-\tau_{mn})\right] \tag{9}$$

for the probability amplitude, where $\theta(t)$ is the Heaviside step function. The derivation of delay differential equations for multiple channels has been investigated in our previous work.[53] We have defined the phase factor $\phi_{mn} = 2k_{mn0}z_0$ and the atomic spontaneous emission rate in TM_{mn} mode

$$\gamma_{mn} = \frac{4d^2\Omega_{mn}^2}{A\varepsilon_0\omega_0\upsilon_{mn}}\sin^2\frac{m\pi}{2}\sin^2\frac{n\pi}{2}. \tag{10}$$

The first term on the right-hand side of Eq. (9) leads to the exponential decay of the atom, the second term involved the delay time τ_{mn} has implied the retarded backaction, which makes this system behave as non-Markovian evolution.

3. Information backflow and the measure for non-Markovianity

Recently, great attention has been paid on the non-Markovian dynamics of open quantum systems, and a number of non-Markovianity measures have been proposed to study the non-Markovian effect quantitatively.[36–38] In general, the measures are not equivalent, and we employ the Breuer, Laine, Piilo (BLP) measure.[37,39,42]

The BLP measure of non-Markovianity is based on the behavior of information backflow between system and environment. Note that the Markovian processes always tend to continuously reduce the trace distance between any pair of states of a quantum system, and this means that the distinguishability between states continues to decrease. On the contrary, an increase of the trace distance implies an increase in the distinguishability between states and the emergence of non-Markovianity. Breuer *et al.* linked the change of the trace distance to the amount of information exchanged between the open system (atom) and its environment (electromagnetic field), and concluded that the quantum memory of a system can be quantified by the non-Markovianity, which is related to the trace distance for quantum states.

The trace distance for quantum states ρ_1 and ρ_2 is defined as $D(\rho_1,\rho_2) = \frac{1}{2}\mathrm{tr}|\rho_1 - \rho_2|$, with $|A| = \sqrt{A^\dagger A}$. For a given pair of initial states $\rho_{1,2}(0)$ of the system, the change of the trace distance is described by

$$\sigma(t,\rho_{1,2}(0)) = \frac{\mathrm{d}}{\mathrm{d}t}D(\rho_1(t),\rho_2(t)), \tag{11}$$

where $\rho_{1,2}(t)$ are the states of the system at time t evolving from the initial states $\rho_{1,2}(0)$. For Markovian processes, the monotonically reduction of the trace distance implies that $\sigma(t,\rho_{1,2}(0)) \le 0$, however, if there exists a pair of initial states of the system such that $\sigma(t,\rho_{1,2}(0)) \ge 0$ at time $t > 0$, then the information flows back from environment to the system, and the process is non-Markovian according to BLP's criterion. Considering that the measure should reveal the total feature of a whole quantum process, they thus define the measure of non-Markovianity of a quantum process as

$$\mathcal{N} = \max_{\rho_{1,2}(0)}\int_{\sigma>0}\mathrm{d}t\,\sigma(t,\rho_{1,2}(0)), \tag{12}$$

where the time integration is extended over all intervals in which σ is positive, and the maximum is taken over all pairs of initial states. For any Markovian process, we have $\mathcal{N} = 0$; if $\mathcal{N} > 0$, the process must be non-Markovian.

To calculate the non-Markovianity from Eq. (12), one should take the maximum over all initial states $\rho_{1,2}(0)$, which is difficult. The authors in Refs. [39–41] provide a strong numerical and theoretical evidence that: for any non-Markovian evolution of a qubit, the optimal pairs of initial states correspond to antipodal points on the equator of the Bloch sphere, in other words, this pair of initial states are orthogonal. For a qubit in amplitude-damping channels, the maximum is attained for the initial states $\rho_1(0) = |e\rangle\langle e|$ and $\rho_2(0) = |g\rangle\langle g|$. This result could have been expected since $|e\rangle\langle e|$ has the maximum initial trace distance from $|g\rangle\langle g|$.[41] The rate of change of the trace distance in a single excitation space is reduced to

$$\sigma(t,\rho_{1,2}(0)) = \frac{\mathrm{d}}{\mathrm{d}t}|e(t)|^2, \tag{13}$$

that is, the trace distance $D(\rho_1(t),\rho_2(t))$ is directly linked to the single-qubit excited-state population $|e(t)|^2$ in the system we analyzed. It means that a return of information from the environment back into the qubit is always accompanied by a feedback of energy.

3.1. Non-Markovianity in the effective single-mode

In this part, we consider the effects of the position of the atom in the effective single-mode case. In the frequency band between Ω_{11} and Ω_{13}, the waveguide is said to be single-moded. The atom with the transition frequency $\omega_0 \in (\Omega_{11},\Omega_{13})$ only emits photons into the TM_{11} mode, the delay-differential equation (9) reduces to

$$\dot{e}(t) = -\frac{\gamma_{11}}{2}e(t) - \frac{\gamma_{11}}{2}\mathrm{e}^{\mathrm{i}\phi_{11}}e(t-\tau_{11})\,\theta(t-\tau_{11}). \quad (14)$$

The derivation of time-delay differential equation is a well-established technique, which has been used in Refs. [46–49, 53] to analyze the influence of delay effect on various physical phenomena in different physical models with single guided mode. By taking the Laplace transform of Eq. (14) and use the geometric series expansion, the analytical solution describing the atomic excitation amplitude can be obtained by the inverse Laplace transform straightforwardly,

$$e(t) = \exp\left(-\frac{\gamma_{11}}{2}t\right)\sum_{n=0}^{\infty}\frac{(f_{11})^n}{n!}(t-n\tau_{11})^n\,\theta(t-n\tau_{11}), \quad (15)$$

where

$$f_{mn} \equiv \frac{\gamma_{mn}}{2}\mathrm{e}^{\mathrm{i}(\phi_{mn}+\pi)}\exp\left(\frac{\gamma_{mn}}{2}\tau_{mn}\right). \quad (16)$$

A half-wave loss during reflection can be observed in Eq. (16) due to an additional π phase difference.

In Eq. (15), the step function $\theta(t-n\tau_{11})$ divides the time axis into intervals of length τ_{11}. For $t\in[0,\tau_{11}]$, the atomic probability $|e(t)|^2 = \mathrm{e}^{-\gamma_{11}t}$ decays exponentially, which coincides with the Markovian behavior of an excited atom in an infinite waveguide. The underlying physics is that the atom requires at least the time τ_{11} that the emitted photon needs to travel back to the atom in order to recognize the mirror. For $t\in[\tau_{11},+\infty)$, the energy carried by the emitted photon is back to the atom, the return wave reflected by the boundary gives rise to the interference with the emitted wave by the atom. When the lifetime of the atom is much longer than the time required for the energy reflow, *i.e.*, $\gamma_{11}\tau_{11}\ll 1$, the atomic probability $|e(t)|^2 \approx \mathrm{e}^{-\gamma_{11}t(1+\cos\phi_{11})}$ is determined by the phase ϕ_{11}. The interference between the emitted wave and the radiation wave reflected back to the atom leads to an enhanced or a decreased decay rate of the atom. When $\phi_{11}=2l\pi$ with integer l, the decay rate increases to $2\gamma_{11}$, when $\phi_{11}=2l\pi+\pi$, the decay rate becomes 0 and the system is fixed in an atom–photon bound state. In Figs. 2(b)–2(d), we have plotted the atomic probability $|e(t)|^2$ as a function of the dimensionless time t/τ_{11}. Since $\phi_{mn}=2k_{mn0}z_0$, the parameters $\gamma_{11}\tau_{11}$ and ϕ_{11} are all determined by the coordinate z_0. For comparison, the exponential decay of the atom inside an infinite waveguide is plotted with the black solid line. An exponential decay law of the atomic probability can be found in Fig. 2(b). Hence, a Markovian process is presented. As z_0 increases to meet $\gamma_{11}\tau_{11}\sim 1$, the atomic probability decays exponentially for $t\in[0,\tau_{11}]$ in Fig. 2(c), however, a behavior deviating from the exponential decay law can be observed after τ_{11}. An increase of the probability appears when $\phi_{11}=2l\pi+\pi$, *i.e.*, energy flows back to the atom which indicates a non-Markovian behavior. As z_0 further increases to meet $\gamma_{11}\tau_{11}\gg 1$ in Fig. 2(d), the atom first decays to the ground state, later, a partial revival of the atomic population can be found. Figures 2(b)–2(d), describing atomic probability in the effective single-mode, are very similar to the conclusion in Refs. [46,53]. The authors in Refs. [46,53] have studied the dynamical evolution of atom interacting with a half-cavity and a semi-infinite rectangular waveguide, respectively.

It is the energy backflow caused by the mirror that generates the non-Markovian behavior. To study the influence of the delay time and phase on the non-Markovian behavior of the quantum dynamics, we have plotted the $\sigma(t)$ as a function of dimensionless time t/τ_{11} in Fig. 3, the regions with positive $\sigma(t)$ represent the intervals of energy backflow. Although the atomic coordinate z_0 determines the magnitudes of the delay time τ_{11} and the phase ϕ_{11}, one can removing the influence of the phase by changing the phase with 2π. In Fig. 3(a), we have plotted $\sigma(t)$ as a function of dimensionless time t/τ_{11} for different $\gamma_{11}\tau_{11}$ to study the effect of the delay time, where we have set $\phi_{11}=2l\pi+\pi$ with different integer l. It can be observed that as $\gamma_{11}\tau_{11}$ increases the number of peaks with $\sigma(t)>0$ increasing, and its maximum value increases too, which indicates that the amount of information backflow becomes larger, so the non-Markovianity increases. In Fig. 3(b), the time derivative of the atomic probability is plotted for different phase when $\gamma_{11}\tau_{11}$ is around 1. The maximum of $\sigma(t)$ appears at $\phi_{11}=2l\pi+\pi$ due to the energy trapped in the atom–mirror interspace, and the minimum of $\sigma(t)$ appears at $\phi_{11}=2l\pi$, after the photon travels a round trip between atom and mirror. Figures 3(a) and 3(b) indicate that both the delay time and phase contribute to the non-Markovian dynamics. However, only the delay time makes contribution to the information backflow in Fig. 3(c) when $\gamma_{11}\tau_{11}\gg 1$. The physics for $\gamma_{11}\tau_{11}\gg 1$ is implied in Fig. 2(d): When the lifetime of the atom is much smaller than the delay time τ_{11}, the atom has already decayed to the ground state before the time that the photon bounces back to the atom. Therefore there is no emitted wave to be interference with the wave reflected back to the atom, which means that the appearance of non-Markovianity comes from the partial re-excitation of atoms. The light emitted in the positive direction has departed from the atom, the probability that the atom is re-excited becomes lower and lower, eventually approaching 0.

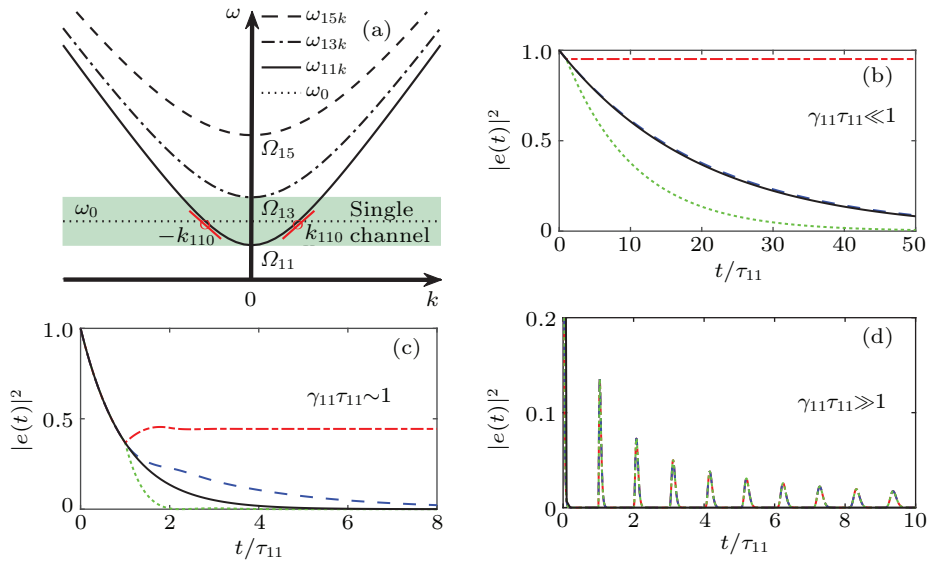


Fig. 2. (a) Schematic illustration for an atom with energy $\omega_0 = (\Omega_{13}+\Omega_{11})/2$ emitting a photon with wave number k_{110} only in the TM_{11} mode. (b)–(d) Atomic excitation probability as a function of t/τ_{11} for the atom is located at (b) $\Gamma_{11}\tau_{11}\sim 0.05$, (c) $\Gamma_{11}\tau_{11}\sim 1$, and (d) $\Gamma_{11}\tau_{11}\sim 50$ with different phases $\phi_{11} = 2l\pi$ (green dotted line), $\phi_{11} = 2l\pi+\pi/2$ (blue dashed line), $\phi_{11} = 2l\pi+\pi$ (red dot-dashed line). We have set the following parameters: $k_{110}v_{11}/\gamma_{11} = 2\pi\times 0.67\times 10^{10}$. The black solid line corresponds to the case when the waveguide is infinite.

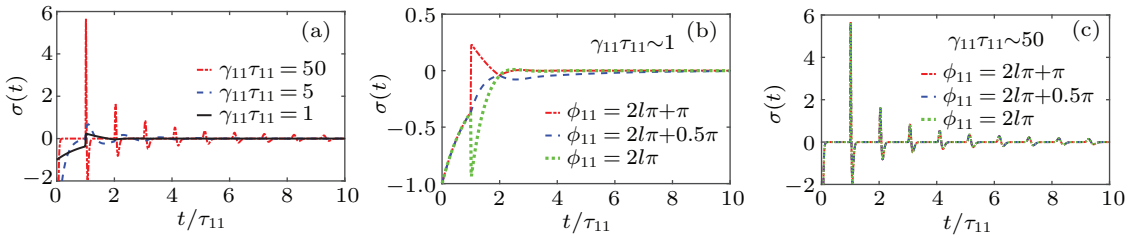


Fig. 3. The rate of change of the trace distance $\sigma(t,\rho_{1,2}(0))$ as a function of the dimensionless time t/τ_{11} (a) for $\gamma_{11}\tau_{11} = 50$ (red dot-dashed line), $\gamma_{11}\tau_{11} = 5$ (blue dashed line), $\gamma_{11}\tau_{11} = 1$ (black solid line), (b) for a given $\gamma_{11}\tau_{11}\sim 1$ and (c) $\gamma_{11}\tau_{11}\sim 50$ but with different phases $\phi_{11} = 2l\pi$ (green dotted line), $\phi_{11} = 2l\pi+\pi/2$ (blue dashed line), $\phi_{11} = 2l\pi+\pi$ (red dot-dashed line). We have set the following parameters: $k_{110}v_{11}/\gamma_{11} = 2\pi\times 0.67\times 10^{10}$.

In the deep non-Markovian regime characterized by $\gamma_{11}\tau_{11}\gg 1$, the influence of phase ϕ_{11} disappears and the atomic probability is simplified as a piecewise function

$$|e(t)|^2 = \mathrm{e}^{-\gamma_{11}t}\left[\frac{\{(\gamma_{11}/2)\exp[(\gamma_{11}/2)\tau_{11}]\}^n}{n!}\right]^2 (t-nt_{11})^{2n}\,\theta(t-nt_{11}), \tag{17}$$

which is in agreement with Fig. 2(d). We can obtain the maximum point $t = n\tau_{11}+2n/\gamma_{11}$ by solving $\sigma(t) = 0$ in the time interval $[n\tau_{11},(n+1)\tau_{11}]$ with integer $n>0$. Then the analytical expression of $\mathcal{N}$ in this deep non-Markovian regime reads

$$\mathcal{N}_{\gamma_{11}\tau_{11}\gg 1} = \sum_{n=1}^{\infty}|e(t)|^2\Big|_{n\tau_{11}}^{n\tau_{11}+2n/\gamma_{11}} = \sum_{n=1}^{\infty}\frac{\mathrm{e}^{-2n}}{(n!)^2}n^{2n} \tag{18}$$

and we find $\mathcal{N}\simeq 0.75$ for $\gamma_{11}\tau_{11}\gg 1$. The mathematical method adopted here is consistent with that in Ref. [47]. In Fig. 4(a), the non-Markovianity $\mathcal{N}$ is plotted numerically as a function of $\gamma_{11}\tau_{11}$. The non-Markovianity has a tendency to increase as $\gamma_{11}\tau_{11}$ grows. However, this increasing is not monotonous. The non-Markovianity is bounded in the grey region, the reason for generating the grey region is that τ_{11} is determined by the distance z_0 and the phase changes rapidly as the distance z_0 varies a little. One can also find that the evolution of the atom is a Markovian process when $\gamma_{11}\tau_{11}\to 0$ and the phases have no effect on the non-Markovianity as $\gamma_{11}\tau_{11}$ becomes larger enough because $\mathcal{N}$ approaches an asymptotic value. It is worth noting that the asymptotic value is a constant independent of all physical quantities of the system. To fit the envelope of the grey region, we also plot the non-Markovianity $\mathcal{N}$ as a function of $\gamma_{11}\tau_{11}$ for phases $\phi_{11} = 2l\pi+\pi$ (the red crosses), $2l\pi+\pi/2$ (the blue squares), $2l\pi$ (the green triangles) in Fig. 4(a) by removing the dependence of the phase on z_0. From Fig. 4(a), we see that in the case $\gamma_{11}\tau_{11}\sim 1$ the regional maximums of $\mathcal{N}$ appear on the envelope line marked by the red crosses with the phases $\phi_{11} = 2l\pi+\pi$. This can be understood as that the process of forming atom–photon bound state in this region is the main source of non-Markovianity $\mathcal{N}$ as shown in Figs. 2(c) and 3(b). As $\gamma_{11}\tau_{11}$ increases, the regional maximums appear on the envelope line marked by the green triangles with the phases $\phi_{11} = 2l\pi$ until the phase effect disappears. In this region, the rapid reabsorptions and reemis-

sions of atom caused by the enhanced atomic decay rate play a major role in information backflowas, as shown in Figs. 2(d) and 3(c).

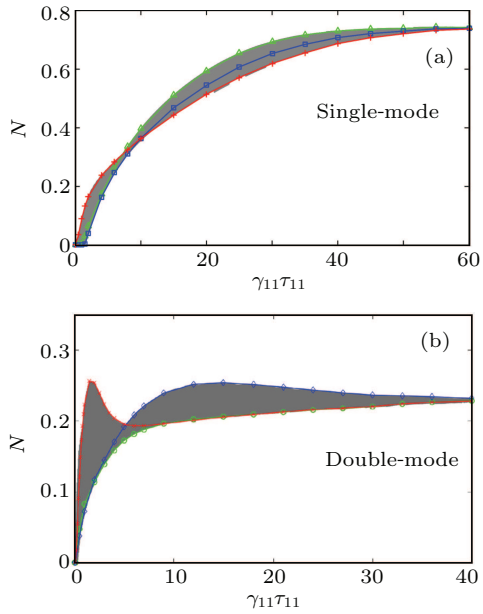


Fig. 4. Non-Markovianity as a function of $\gamma_{11}\tau_{11}$ for (a) one TM mode with parameters: $k_{110}v_{11}/\gamma_{11} = 2\pi \times 0.67 \times 10^{10}$, and (b) two TM modes with parameters: $k_{110}v_{11}/\gamma_{11} = 2\pi \times 9.1 \times 10^{10}$. (a) Phases $\phi_{11} = 2l\pi + \pi$ (the red crosses), $2l\pi + \pi/2$ (the blue squares), $2l\pi$ (the green triangles) by removing the dependence of the phase on z_0; (b) phases $\phi_{11} + \pi = 290l'\pi$ (the red crosses), $145l'\pi$ (the blue diamonds), $290l'\pi + 2.45\pi$ (the green circles) by removing the dependence of the phase on z_0.

3.2. Non-Markovianity in the effective double-modes

An excited atom radiates waves into all modes of propagation that resonate with itself. According to the dispersion relation, as the cross-sectional area becomes larger, more propagation modes are involved in the resonance with the atom. Different group velocities v_{mn} introduce corresponding delay time τ_{mn} required for a photon propagating in the TM_{mn} mode to be reabsorbed by the atom. In this part, we assume that the atomic transition frequency is in the regime $(\Omega_{13}, \Omega_{15})$ but far away from the cutoff frequencies, *i.e.*, two effective modes (TM_{11} amd TM_{13}) is in resonance with the atom. The delay-differential equation (9) becomes

$$\begin{aligned}\dot{e}(t) = &-\frac{\gamma_{11}+\gamma_{13}}{2}e(t)\\ &-\frac{\gamma_{11}}{2}\mathrm{e}^{\mathrm{i}\phi_{11}}e(t-\tau_{11})\,\theta(t-\tau_{11})\\ &-\frac{\gamma_{13}}{2}\mathrm{e}^{\mathrm{i}\phi_{13}}e(t-\tau_{13})\,\theta(t-\tau_{13}),\end{aligned} \tag{19}$$

where τ_{13} is the delay time and ϕ_{13} is the phase in TM_{13} mode due to the photon reflected at the mirror at $z = 0$ to the atom. In Eq. (19), the step functions $\theta(t - n\tau_{11})$ and $\theta(t - n\tau_{13})$ divide the time axis of two guided modes into intervals of length τ_{11} and τ_{13}, respectively. We note that the multichannel delay times $\tau_{mn} = 2z_0/v_{mn} = 2z_0\omega_0/c^2k_{mn0}$ and the phase factors $\phi_{mn} = 2k_{mn0}z_0$ caused by the rectangular waveguide are dependent on the dispersion relation, as shown in Fig. 5(a). Both the delay times $\tau_{11} < \tau_{13}$ and the phases $\phi_{11} > \phi_{13}$ are all modulated by atomic coordinate z_0, $\gamma_{11} < \gamma_{13}$. When $\gamma_{13}\tau_{13} \to 0$, the atomic probability

$$|e(t)|^2 = \exp\left[-\gamma_{11}t\,(1+\cos\phi_{11}) - \gamma_{13}t\,(1+\cos\phi_{13})\right], \tag{20}$$

which presents a Markovian dynamics. Comparing to the effective single-mode case, the decay rate of the atom is enhanced. Equation (20) indicates that phases are important for the decay rate of the atom when the atom is close to the termination of the waveguide.

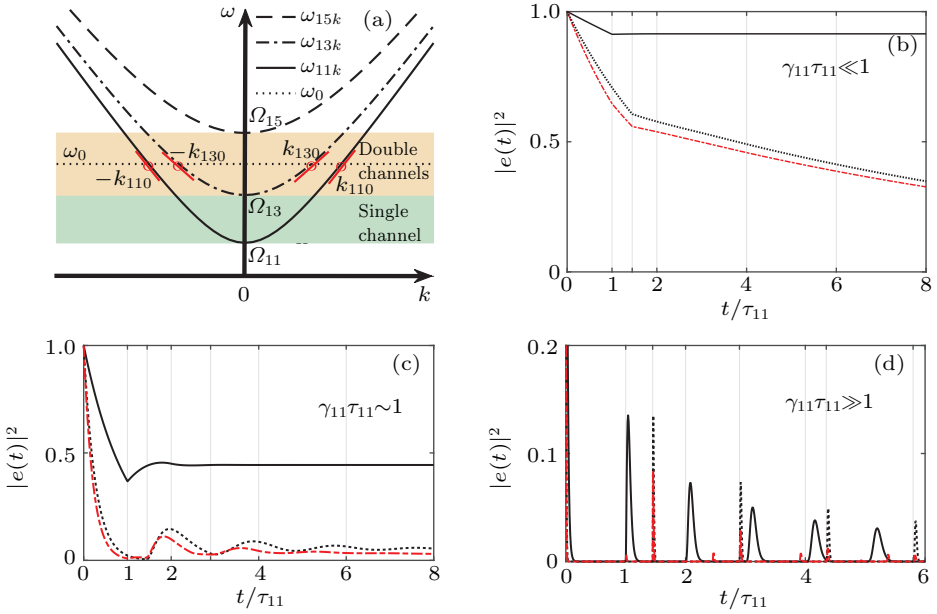


Fig. 5. (a) Schematic illustration for an atom with energy $\omega_0 = (\Omega_{13} + \Omega_{15})/2$ emitting a photon with wave numbers k_{110} and k_{130} in the TM_{11} and TM_{13} modes respectively. (b)–(d) Atomic excitation probability as a function of the dimensionless time t/τ_{11} for $\gamma_{11}\tau_{11} \ll 1$ but $\gamma_{13}\tau_{13} \sim 1$ (b), $\gamma_{11}\tau_{11} \sim 1$ (c), and $\gamma_{11}\tau_{11} \sim 50$ (d) with the phase $\phi_{11} = 2l\pi + \pi$ (red dot-dashed line). We have set the following parameters: $k_{110}v_{11}/\gamma_{11} = 2\pi \times 9.1 \times 10^{10}$. For comparisons, we have also drawn the atomic excitation probability by only considering the TM_{11} mode (black solid line) and TM_{13} mode (black dotted line), respectively.

By the Laplace transform and the geometric series expansion, the time behavior of atomic excitation amplitude reads

$$e(t) = \exp\left(-\frac{\gamma_{11}+\gamma_{13}}{2}t\right)\sum_{n,m=0}^{\infty}\frac{(f_{11})^n(f_{13})^m}{n!m!} \times \exp\left(\frac{\gamma_{13}}{2}n\tau_{11}\right)\exp\left(\frac{\gamma_{11}}{2}m\tau_{13}\right) \times (t-n\tau_{11}-m\tau_{13})^{n+m}\,\theta(t-n\tau_{11}-m\tau_{13}). \quad (21)$$

From the step function $\theta(t-n\tau_{11}-m\tau_{13})$ in Eq. (21), it can be seen that the two effective modes cannot be decomposed into two completely independent single-modes. We can interpret it as follows: photon can be repeatedly transformed between two feedback channels through repeated interactions with atom, so the two non-interacting channels become inseparable due to repeated emission and absorption of atom.

In the interval $[0,\tau_{11}]$, the atomic probability $|e(t)|^2 \approx \mathrm{e}^{-(\gamma_{11}+\gamma_{13})t}$ decays with rate $\gamma_{11}+\gamma_{13}$. After time τ_{11}, the interference caused by phase ϕ_{11} takes effect, phase ϕ_{13} does not play the role until the time $t>\tau_{13}$ that the atom recognizes the mirror in the channel formed by the TM_{13} mode. Therefore, the dimensionless parameters $\gamma_{11}\tau_{11}$, $\gamma_{13}\tau_{13}$ distinguish the Markovian region from the non-Markovian region of the two channels. In Figs. 5(b)–5(d), we have plotted the atomic probability $|e(t)|^2$ as a function of the dimensionless time t/τ_{11} by keeping the phase $\phi_{11}=2l\pi+\pi$ for different $\gamma_{11}\tau_{11}$. For comparisons, we have also plotted $|e(t)|^2$ by only considering the TM_{11} mode (black solid line) and TM_{13} mode (black dotted line), respectively. It can be found in Fig. 5(b) that the atom–photon bound state cannot be formed since the energy loses from the atom when $\gamma_{11}\tau_{11}\ll 1$. There is an arrival of the energy to the atom by the TM_{13} mode when $\gamma_{11}\tau_{11}\sim 1$ in Fig. 5(c). In the region $\gamma_{11}\tau_{11}\gg 1$ ($\gamma_{13}\tau_{13}>\gamma_{11}\tau_{11}$), the atom has already decayed to the ground state when the wave reflected by the boundary returns to the atom. The collapses and partial revivals of the atomic probability appear in Fig. 5(d). This behavior is similar to Fig. 2(d), both phase-independent, but unlike the effective single-mode case, the time points of the atom's revivals occur at $(n\tau_{11}+m\tau_{13})$. It is worth noting that the peaks of atomic re-excitation in Fig. 5(d) are not decrease sequentially. This phenomenon is due to the different decay rates resulting in different energy carried between the channels. Since $\gamma_{13}/\gamma_{11}=\Omega_{13}^2k_{110}\Omega_{11}^2k_{130}>1$, the atom rapidly radiates energy into the TM_{13} mode, the energy backflow through the TM_{13} is greater than that of the TM_{11} mode as shown in Eq. (16).

In Fig. 6, we have also plotted the change of the trace distance $\sigma(t,\rho_{1,2}(0))$ as a function of t/τ_{11} in the effective double-modes. In Fig. 6(a), we have plotted $\sigma(t)$ as a function of dimensionless time t/τ_{11} to study the effect of the delay time. This shows that the two-modes case enters the non-Markovian region earlier than the single-mode case. Different from that in Fig. 3(b), multiple extremum can be observed for any fixed phase in Fig. 5(b), these extremums are generated by the interference of the emitted wave and the propagating wave in It can be found that the effect of phases become less and less as the distance between the atom and the mirror increases, however the energy flows back and forth between the atom and the waveguide which are completely characterized by the delay times as the atom is far way from the mirror.

In Fig. 4(b), the non-Markovianity $\mathcal{N}$ is plotted numerically as a function of $\gamma_{11}\tau_{11}$ for two TM modes. Similarly, we first give an analytical analysis of the non-Markovianity of the system in the deep Markovian regime. Owing to the long delay time, the light reflected back from the boundary cannot recombine with the light emitted by the atom, and no interference can occur. At this point, the phases ϕ_{mn} no longer affect the non-Markovian dynamics of the system. Therefore, the atomic probability reduces to a piecewise function

$$|e(t)|^2 = \mathrm{e}^{-(\gamma_{11}+\gamma_{13})t}\left[\frac{\left(\frac{\gamma_{11}}{2}\right)^n\left(\frac{\gamma_{13}}{2}\right)^m}{n!m!}\right]^2 \mathrm{e}^{(\gamma_{11}+\gamma_{13})(n\tau_{11}+m\tau_{13})}(t-n\tau_{11}-m\tau_{13})^{2n+2m}\,\theta(t-n\tau_{11}-m\tau_{13}) \quad (22)$$

in each time interval of unequal length divided by two delay times. The maximum point $t=n\tau_{11}+m\tau_{13}+(2n+2m)/(\gamma_{11}+\gamma_{13})$ can be obtained by solving $\sigma(t)=0$ in each time interval. Then the analytical expression of $\mathcal{N}$ in the effective double-modes reads

$$\mathcal{N}_{\gamma_{11}\tau_{11}\gg 1} = \sum_{n,m=0}^{\infty}|e(t)|^2\Big|_{n\tau_{11}+m\tau_{13}}^{\frac{2n+2m}{\gamma_{11}+\gamma_{13}}+n\tau_{11}+m\tau_{13}} - 1 = \sum_{n,m=0}^{\infty}\frac{\mathrm{e}^{-(2n+2m)}(n+m)^{2n+2m}}{(n!m!)^2}\frac{(\gamma_{13}/\gamma_{11})^{2m}}{(1+\gamma_{13}/\gamma_{11})^{2n+2m}} - 1. \quad (23)$$

Unlike the effective single-mode case, the limit value of $\mathcal{N}$ in the effective two-modes case is no longer a constant, but depends on the relative parameters γ_{13}/γ_{11} of the two modes. This fully demonstrates that the multi-modes case is not a straightforward generalization of the effective single-mode. As shown in Eq. (21), two non-interacting channels become non-decomposable through atom. Multiple energy backflow channels provide a possible platform for controllable non-Markovianity. Under the parameters we considered, the analytical result is $\mathcal{N}_{\gamma_{11}\tau_{11}\gg 1}\simeq 0.23$ after calculations, which is

consistent with the numerical analysis in Fig. 4(b). In addition to the deep Markovian regime $\gamma_{11}\tau_{11} \gg 1$, figure 4(b) also shows that $\mathcal{N}$ does not increases monotonously with $\gamma_{11}\tau_{11}$ increases. As z_0 increases, the phase factors ϕ_{11} and ϕ_{13} oscillate rapidly, so $\mathcal{N}$ is also bounded in the grey region. When the delay time τ_{11} is comparable to the lifetime γ_{11}^{-1}, $\mathcal{N}$ increases much larger in comparison to that of the effective single-mode. Its physical origin is that $\gamma_{13}/\gamma_{11} > 1$ causes the system to enter the non-Markovian regime earlier when $\tau_{13} \sim \gamma_{13}^{-1}$. However, an asymptotic value of $\mathcal{N}$ as $\gamma_{11}\tau_{11}$ is larger enough is lower than that of the single transverse mode since energy loses much faster and flows away from the atom to the open port of the waveguide. To found the envelope of the grey region, we also plot $\mathcal{N}$ as a function of $\gamma_{11}\tau_{11}$ for given phases by removing the dependence of φ_{11} on the atom–mirror distance, where the phase in the TM_{13} mode is also determined by ϕ_{11} via $\phi_{13} = \phi_{11}\sqrt{\omega_0^2 - \Omega_{13}^2}/\sqrt{\omega_0^2 - \Omega_{11}^2}$.

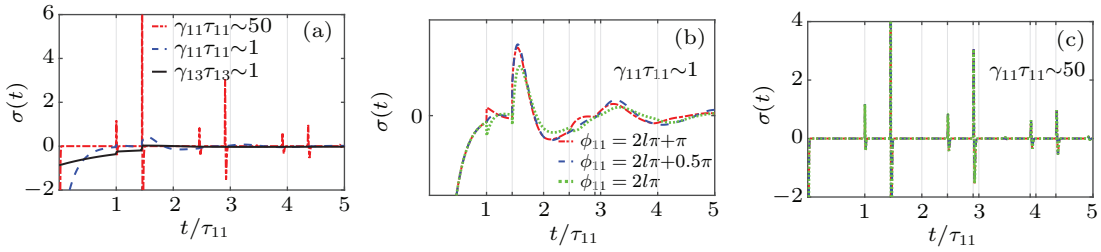


Fig. 6. The change of the trace distance $\sigma(t, \rho_{1,2}(0))$ as a function of t/τ_{11} in double transverse modes for (a) different $\gamma_{11}\tau_{11}$ are chosen, (b) $\gamma_{11}\tau_{11} \sim 1$ but different phases, (c) fixed $\gamma_{11}\tau_{11} \sim 50$ with $\phi_{11} = 2l\pi + \pi$ (red dot-dashed line), $\phi_{11} = 2l\pi + 0.5\pi$ (blue dashed line), $\phi_{11} = 2l\pi$ (green dotted line). We have set the following parameters: $k_{110}v_{11}/\gamma_{11} = 2\pi \times 9.1 \times 10^{10}$.

4. Discussion and conclusion

We studied the influence of the atom–mirror distance on the non-Markovianity $\mathcal{N}$ of an two-level atom coupled to a semi-infinite rectangular hollow metallic waveguide, where the finite end is assumed to be a perfect mirror which force part of the emitted light back to the atom. The TM_{mn} transverse modes are picked out to interact with the atom by restricting the direction of the atom's dipole. When the energy separation of the atom is far away from the cutoff frequencies of the transverse modes and there is single excitation in the total system, the dynamics of the atom is described by the delay differential equation, which are characterized by the lifetime of the atom and the atom–mirror distance. The delay differential equations are solved exactly for the atom interacting with either single transverse mode or double transverse modes of the waveguide. Although the atom–mirror distance introduces the phase factors ϕ_{mn} and delay times τ_{mn}, the environmental memory time is characterized by the delay times that required for light to travel a round trip between atom and mirror in the transverse modes. When the atom radiates energy into single TM mode of the waveguide, the atom–photon bound state can be found when the lifetime γ_{11}^{-1} is larger than the delay time τ_{11}, $\mathcal{N}$ increases as the atom–mirror distance increases, and approaches an asymptotic value as the atom–mirror distance becomes larger enough. However, the information backflow imposed by a geometrical confinement of the field becomes complicated when the atom radiating into double TM modes of the waveguide. The atom–photon bound state disappears. There is an increasing of $\mathcal{N}$ induced by the interference between the wave reflected by the boundary and the emitted wave by the atom when the delay times is comparable to the lifetime, however, the asymptotic value of $\mathcal{N}$ is lower than that of the single transverse mode. Via a numerical approach, the non-Markovianity is found to occur in a finite region. The non-Markovian boundary of each channel occurs at $\gamma_{mn}\tau_{mn} \sim 1$. In the deep Markovian regime, the limit value of the non-Markovianity $\mathcal{N}$ in the multimodes case is related to the relative decay rates of the multichannels, a phenomenon that does not occur in the single-mode case. It is worth noting that the parameters choice in this paper correspond to the experimental setup of the interaction of natural atom with microwave waveguide.[48,52,55]

Acknowledgements

Project supported by the National Natural Science Foundation of China (Grant Nos. 11935006, 12075082, 12205088, and 11975095), the Science and Technology Innovation Program of Hunan Province, China (Grant No. 2020RC4047), the Scientific Research Fund of the Hunan Provincial Education Department (Grant No. 21B0639), and Hunan Normal University Open Foundation of Key Laboratory of Low-Dimensional Quantum Structures and Quantum Control of the Ministry of Education (Grant No. QSQC2009).

References

[1] Shen J T and Fan S 2005 *Opt. Lett.* **30** 2001
[2] Shen J T and Fan S 2005 *Phys. Rev. Lett.* **95** 213001
[3] Kimble H J 2008 *Nature* **453** 1023
[4] Dayan B, Parkins A S, Aoki T, Ostby E P, Vahala K J and Kimble H J 2008 *Science* **319** 1062
[5] Zhou L, Gong Z R, Liu Y X, Sun C P and Nori F 2008 *Phys. Rev. Lett.* **101** 100501
[6] Roy D, Wilson C M and Firstenberg O 2017 *Rev. Mod. Phys.* **89** 021001

[7] Hoi I C, Wilson C M, Johansson G, Palomaki T, Peropadre B and Delsing P 2011 *Phys. Rev. Lett.* **107** 073601
[8] Zhou L, Yang L P, Li Y and Sun C P 2013 *Phys. Rev. Lett.* **111** 103604
[9] Tiecke T G, Thompson J D, Leon N P, Liu L R, Vuletić V and Lukin M D 2014 *Nature* **508** 241
[10] Shomroni I, Rosenblum S, Lovsky Y, Bechler O, Guendelman G and Dayan B 2014 *Science* **345** 903
[11] García-Álvarez L, Casanova J, Mezzacapo A, Egusquiza I L, Lamata L, Romero G and Solano E 2015 *Phys. Rev. Lett.* **114** 070502
[12] Bajcsy M, Hofferberth S, Balic V, Peyronel T, Hafezi M, Zibrov A S, Vuletic V and Lukin M D 2009 *Phys. Rev. Lett.* **102** 203902
[13] Babinec T M, Hausmann B J, Khan M, Zhang Y, Maze J R, Hemmer P R and Lončar M 2010 *Nat. Nanotechnology* **5** 195
[14] Arcari M, Söllner I, Javadi A, Lindskov Hansen S, Mahmoodian S, Liu J, Thyrrestrup H, Lee E H, Song J D, Stobbe S and Lodahl P 2014 *Phys. Rev. Lett.* **113** 093603
[15] Lund-Hansen T, Stobbe S, Julsgaard B, Thyrrestrup H, Sünner T, Kamp M, Forchel A and Lodahl P 2008 *Phys. Rev. Lett.* **101** 113903
[16] Laucht A, Pütz S, Günthner T, Hauke N, Saive R, Frédérick S, Bichler M, Amann M C, Holleitner A W, Kaniber M and Finley J J 2012 *Phys. Rev. X* **2** 011014
[17] Goban A, Hung C L, Yu S P, Hood J D, Muniz J A, Lee J H, Martin M J, McClung A C, Choi K S, Chang D E, Painter O and Kimble H J 2014 *Nat. Commun.* **5** 3808
[18] Huck A and Andersen U L 2016 *Nanophotonics* **5** 483
[19] Akimov A V, Mukherjee A, Yu C L, Chang D E, Zibrov A S, Hemmer P R, Park H and Lukin M D 2007 *Nature* **450** 402
[20] Akselrod G M, Argyropoulos C, Hoang T B, Ciracì C, Fang C, Huang J, David R S and Mikkelsen M H 2014 *Nat. Photon.* **8** 835
[21] Astafiev O, Zagoskin A M, Abdumalikov A A, Pashkin Y A, Yamamoto T, Inomata K, Nakamura Y and Tsai J S 2010 *Science* **327** 840
[22] Astafiev O V, Abdumalikov A A, Zagoskin A M, Pashkin Y A, Nakamura Y and Tsai J S 2010 *Phys. Rev. Lett.* **104** 183603
[23] Abdumalikov A A, Astafiev O, Zagoskin A M, Pashkin Y A, Nakamura Y and Tsai J S 2010 *Phys. Rev. Lett.* **104** 193601
[24] Hoi I C, Palomaki T, Lindkvist J, Johansson G, Delsing P and Wilson C M 2012 *Phys. Rev. Lett.* **108** 263601
[25] Hoi I C, Kockum A F, Palomaki T, Stace T M, Fan B, Tornberg L, Sathyamoorthy S R, Johansson G, Delsing P and Wilson C M 2013 *Phys. Rev. Lett.* **111** 053601
[26] Hoi I C, Wilson C M, Johansson G, Lindkvist J, Peropadre B, Palomaki T and Delsing P 2013 *New. J. Phys.* **15** 025011
[27] Van Loo A F, Fedorov A, Lalumière K, Sanders B C, Blais A and Wallraff A 2013 *Science* **342** 1494
[28] Gu X, Kockum A F, Miranowicz A, Liu Y X and Nori F 2017 *Phys. Rep.* **718** 1
[29] Dirac P A M 1927 *Proc. Roy. Soc. A* **114** 767
[30] Purcell E M *Confined Electrons and Photons* 839
[31] Kleppner D 1981 *Phys. Rev. Lett.* **47** 233
[32] Meschede D 1992 *Phys. Rep.* **211** 201
[33] Li J G, Zou J and Shao B 2010 *Phys. Rev. A* **81** 062124
[34] Zeng H S, Tang N, Zheng Y P and Wang G Y 2011 *Phys. Rev. A* **84** 032118
[35] Zeng H S, Tang N, Zheng Y P and Xu T T 2012 *Eur. Phys. J. D* **66** 255
[36] Rivas Á, Huelga S F and Plenio M B 2014 *Rep. Prog. Phys.* **77** 094001
[37] Breuer H P, Laine E M, Piilo J and Vacchini B 2016 *Rev. Mod. Phys.* **88** 021002
[38] De Vega I and Alonso D 2017 *Rev. Mod. Phys.* **89** 015001
[39] Breuer H P, Laine E M and Piilo J 2009 *Rev. Rev. Lett.* **103** 210401
[40] Laine E M, Piilo J and Breuer H P 2010 *Rev. Rev. A* **81** 062115
[41] Wißmann S, Karlsson A, Laine E M, Piilo J and Breuer H P 2012 *Rev. Rev. A* **86** 062108
[42] Breuer H P 2012 *J. Phys. B: At. Mol. Opt. Phys.* **45** 154001
[43] Ask A and Johansson G 2022 *Phys. Rev. Lett.* **128** 083603
[44] Finsterhölzl R, Katzer M and Carmele A 2020 *Phys. Rev. B* **102** 174309
[45] Fang Y L, Ciccarello F and Baranger H U 2018 *New. J. Phys.* **20** 043035
[46] Tufarelli T, Ciccarello F and Kim M S 2013 *Phys. Rev. A* **87** 013820
[47] Tufarelli T, Kim M S and Ciccarello F 2014 *Phys. Rev. A* **90** 012113
[48] Cook R J and Milonni P W 1987 *Phys. Rev. A* **35** 5081
[49] Dorner U and Zoller P 2002 *Phys. Rev. A* **66** 023816
[50] Huang J F, Shi T, Sun C P and Nori F 2013 *Phys. Rev. A* **88** 013836
[51] Li Q, Zhou L and Sun C P 2014 *Phys. Rev. A* **89** 063810
[52] Hu L J, Lu G Y, Lu J and Zhou L 2020 *Quantum Inf. Process.* **19** 81
[53] Song H X, Sun X Q, Lu J and Zhou L 2018 *Commun. Theor. Phys.* **69** 59
[54] Li J, Hu L J, Lu J and Zhou L 2021 *Chin. Phys. B* **30** 090307
[55] Raimond J M, Brune M and Haroche S 2001 *Rev. Mod. Phys.* **73** 565